



**CHALMERS**  
UNIVERSITY OF TECHNOLOGY

## **Effect of alkalinity on the diffusion of solvent-fractionated lignin through cellulose membranes**

Downloaded from: <https://research.chalmers.se>, 2024-03-13 10:22 UTC

Citation for the original published paper (version of record):

Ghaffari, R., Almqvist, H., Idström, A. et al (2023). Effect of alkalinity on the diffusion of solvent-fractionated lignin through cellulose membranes. *Cellulose*, 30(6): 3685-3698.  
<http://dx.doi.org/10.1007/s10570-023-05098-8>

N.B. When citing this work, cite the original published paper.



# Effect of alkalinity on the diffusion of solvent-fractionated lignin through cellulose membranes

Roujin Ghaffari · Henrik Almqvist · Alexander Idström · Ioanna Sapouna · Lars Evenäs · Gunnar Lidén · Martin Lawoko · Anette Larsson

Received: 4 October 2022 / Accepted: 11 February 2023  
© The Author(s) 2023

**Abstract** Mass transport of liberated lignin fragments from pits and fiber walls into black liquor is considered a determining step in the delignification process. However, our current understanding of the diffusion of lignin through cellulose and the influential parameter on this process is very limited. A comprehensive and detailed study of lignin mass transport through cellulosic materials is, therefore, of great importance. In this study, diffusion cell methodology is implemented to systematically investigate the transport of fractionated kraft lignin molecules through model cellulose membranes. Pulping is a complex process and lignin is very heterogenous material

therefore to perform a more detailed study on lignin diffusion, we included an additional solvent fractionation step. One of the benefits of this method is that the setup can be adjusted to various experimental conditions allowing the complex chemical reactions occurring during pulping, which would affect the mass transfer of lignin, to be avoided. Here, the effects of the alkalinity of the aqueous solution and molecular weight of the kraft lignin molecules on their diffusion were investigated. Additionally, NMR spectroscopy, size exclusion chromatography, and UV/Vis spectroscopy were used to characterize the starting material and the molecules that passed through the membrane. Lignin molecules detected in the acceptor chamber of the diffusion cells had lower molecular weights, indicating a size fractionation between the donor and

**Supplementary Information** The online version contains supplementary material available at <https://doi.org/10.1007/s10570-023-05098-8>.

R. Ghaffari (✉) · A. Idström · L. Evenäs · A. Larsson  
Department of Chemistry and Chemical Engineering,  
Chalmers University of Technology, Gothenburg, Sweden  
e-mail: roujin@chalmers.se

R. Ghaffari · L. Evenäs · A. Larsson  
Wallenberg Wood Science Center, Chalmers University  
of Technology, Gothenburg, Sweden

H. Almqvist · G. Lidén  
Department of Chemical Engineering, Lund University,  
Lund, Sweden

I. Sapouna  
Division of Glycoscience, Department of Chemistry,  
KTH Royal Institute of Technology, AlbaNova University  
Center, Stockholm, Sweden

I. Sapouna · M. Lawoko  
Wallenberg Wood Science Center, KTH Royal Institute  
of Technology, Stockholm, Sweden

L. Evenäs · A. Larsson  
Department of Chemistry and Chemical Engineering,  
FibRe – Centre for Lignocellulose-based Thermoplastics,  
Chalmers University of Technology, Gothenburg, Sweden

M. Lawoko  
Department of Fibre and Polymer Technology, KTH Royal  
Institute of Technology, Stockholm, Sweden

acceptor chamber. UV/Vis showed higher concentrations of ionized conjugated kraft lignin molecules in the acceptor chamber, which is a sign of chemical fractionation. This study suggests that the diffusion of lignin through small cellulose pores can be enhanced by decreasing the average molecular weight of the diffusing kraft lignin molecules and increasing alkalinity.

**Keywords** Lignin · Lignin transport · Kraft process · Diffusion cells

## Introduction

Many methods targeting the removal of one or more of the main macromolecular constituents of biomass, based on strong alkaline or acidic reagents, have been industrialized over the years (Sixta 2006). In chemical pulping, for example, the goal is to remove lignin with as little degradation of carbohydrates as possible (Favis et al. 1981). Conventional kraft pulping is the most utilized industrial chemical pulping method. The initial step of kraft pulping is the impregnation of wood chips with cooking liquor. Once transported into the wood chips, the cooking chemicals react with the lignin and polysaccharides in the wood matrix and form degradation products that gradually diffuse into the bulk liquor (Bogren et al. 2007). It has been shown that longer cooking times at elevated temperatures provide higher delignification rates and increased carbohydrate degradation (Gierer 1980). Meanwhile, the average molecular weight of lignin in the black liquor increases for two main reasons: (i) the solubilized lignin molecules condense, which leads to an increase in the molecular weight of lignin in the free liquor (Komatsu and Yokoyama 2021) and (ii) larger lignin molecules diffuse out of the wood matrix into the free liquor (Mattsson et al. 2017). The diffusion of ions and cooking chemicals into wood chips has been studied in the literature (Birch et al. 1999; Kolavali and Theliander 2013). Although the chemical reactions and their kinetics during pulping have been reported in studies over the years (Lindgren and Lindström 1996; Bogren et al. 2007), few studies have focused on the transport of the degraded lignin out of the wood matrix.

In 1981, Favis et al. suggested that the rate of lignin removal from unbleached pulp in aqueous

solutions is controlled by the diffusion of the lignin macromolecules (Favis et al. 1981). In 1993, it was shown by Li et al. that the leaching of lignin is enhanced by increasing the temperature from 100 to 140 °C and increasing the alkalinity of the solution from 0.1 to 1 M NaOH. They proposed that alkalinity affects the association of degraded lignin molecules, providing a higher diffusivity and faster transport through the fibers (Li and Macleod 1993). Later, the same authors investigated the effect of pH and ionic strength on the leaching of lignin, concluding that lignin diffusion can be affected by pores sizes, molecular sizes, and electrostatic interactions between the fibers and lignin (Li et al. 1997). More recently, the importance of mass transfer of lignin in pulping was presented by Mattsson et al. (2017) who showed that most of the delignification reactions are completed within 20 min from the start of the cooking. However, cooking is required for a longer period to observe the degraded products in the free bulk liquor. This is in line with the study by Brännvall and Rönnols (2021) where the lignin content of free and entrapped liquor in the lumen was investigated. The content of lignin available in the lumen liquor was higher than in the free liquor. They showed that the slowest mass transport rate during cooking is the transport of dissolved lignin from the lumen liquor to the free liquor through fibers.

Based on these studies, the overall delignification process is diffusion-controlled (Favis et al. 1981; Gustafson 1988; Li and Macleod 1993; Li et al. 1997), with the transport of degraded lignin macromolecules out of the cellulose matrix being the rate-determining step. The importance of mass transfer of lignin out of the biomass matrix is not limited to kraft pulping; a kinetics study by Kawamata et al. (2019) showed that the rate-limiting step in organosolv treatment of cedarwood is the diffusion through the cellulose layer.

A low concentration of residual lignin in unbleached pulp, with a minimum loss of carbohydrates, is generally desirable, therefore, the cooking time should be as short as possible. Given the importance of the lignin mass transfer rate to the overall rate of delignification, physicochemical factors that may affect mass transfer need to be understood. Diffusion events of degraded lignin through fibers can be accelerated through (i) a decrease in molecular weight and hydrodynamic radius of the molecules/aggregations, (ii) an increase in the

membrane pore size, which would influence the diffusivity of the molecules, and (iii) a reduction in the attractive interactions between lignin and the membrane or fiber walls (Li and Macleod 1993).

It is known that lignin molecules self-associate, potentially affecting the apparent molecular weight and slowing down the diffusion of lignin molecules. The lignin association process is affected by the concentration of lignin (Rudatin et al. 1989), the ionic strength (Norgren et al. 2001, 2002), and the alkalinity of the solution (Vainio et al. 2004). Higher alkalinity reduces the association and a higher concentration of lignin or salts in the solution increases the association. Additionally, the association process is reversible. (Dutta et al. 1989).

A comprehensive study of how different specific properties of the solution or the lignin molecules can affect lignin mass transport is of great importance. Pulping is a complex process, and several aspects can affect lignin diffusion, such as the presence of polysaccharides, condensation reactions, or degradation of carbohydrates during cooking. The molecular weight and pore sizes vary within different stages of the pulping. To systematically study the effect of molecular weight on the lignin mass transfer in different alkalinity we have design an experimental system based on diffusion cells. To minimize the effect of complex chemical reactions taking place during pulping on mass transfer, already degraded lignin molecules (well characterized solvent fractionated kraft lignin) were used in this study. These lignin fractions have less variance in chemical structures and size than unfractionated lignin molecules. The pore size of the membranes used here are chosen in way to mimic the size of the smallest confinement that lignin needs to pass through in pulping, which is the distances between bundles of microfibril in the cell wall. The lignin samples were characterized using pulsed-field gradient  $^1\text{H}$ -NMR spectroscopy,  $^{31}\text{P}$ -NMR spectroscopy, UV/Vis spectrophotometry, and size exclusion chromatography (SEC).

## Experimental section

### Materials

Softwood kraft lignin (KL), extracted through LignoBoost™ technology, was provided by Stora Enso

kraft pulp mill (Karlstadt, Sweden). The KL was dissolved in alkaline solutions, made by the dissolution of sodium hydroxide pellets (Sigma Aldrich, Germany) in deionized water. Regenerated cellulose (RC) membranes (Spectrum™ Labs Spectra/Por™ Darmstadt, Germany, 50 kDa molecular weight cut-off (MWCO)) were used in the diffusion cells. For the solvent fractionation of KL, ethyl acetate and methanol were purchased from Sigma Aldrich (Germany). Ethanol and acetone were of analytical grade, both purchased from VWR (Möndal, Sweden) samples were filtered by a grade 2 filter paper (Munktell, Sweden). All chemicals used for  $^{31}\text{P}$ -NMR analysis, Dimethylformamide (DMF), pyridine, endo-N-Hydroxy-5-norbornene-2,3-dicarboximide (eHNDI), chromium (III) acetylacetonate, 2-chloro-4,4,5,5-tetramethyl-1,3,2-dioxaphospholane, chloroform- $d_1$ , were purchased from Sigma Aldrich (Germany). Deuterium oxide (99.9 atom % D, Sigma Aldrich, Darmstadt, Germany), and DMSO- $d_6$  (99.9 atom % D, VWR chemicals) were used for diffusion NMR analysis. Water permeation measurements were performed using 5 mCi (185 MBq) tritium-labeled water (PerkinElmer, USA). Ultima Gold (Perkin-Elmer, USA) was added to radio-diffusivity samples prior to measurements.

### Fractionation of softwood KL

Sequential solvent fractionation of the softwood KL was performed according to a protocol previously introduced by Duval et al. (2016). Four solvents were used in the following order: ethyl acetate, ethanol, methanol, and acetone. The solvents were carefully selected by Duval et al by considering the solution yield and the molecular weight distribution of the dissolved lignin in each solvent. It is expected that the molecular weight of the fractions increases from KL1 to KL5.

Twenty gram of KL were initially dispersed in 200 mL ethyl acetate and the solution was stirred for 2 h at room temperature. The soluble and insoluble parts were then separated using grade 2 filter paper. The soluble fraction was concentrated using a rotary evaporator and, after solvent removal, the soluble fraction was redispersed in deionized water and dried by freeze-drying. The insoluble fraction was redispersed in the next solvent and the same procedure was

repeated for all remaining solvents. Figure 1 summarizes the process.

### Pulsed-field gradient NMR spectroscopy

Samples were prepared by dissolving 50 mg of lignin samples in 1 mL of DMSO- $d_6$ . The self-diffusion coefficients,  $D$ , of the different fractions were studied using an AVANCE III HD Bruker NMR spectrometer, operating at 14.1 T, equipped with a 5 mm diff30 probe connected to a 60 A amplifier. Measurements were conducted at 298 K and the temperature was calibrated using pure methanol prior to the experiments (Raiford et al. 1979).

For the  $^1\text{H}$  experiments, a  $15.8\ \mu\text{s}$   $^1\text{H}$ -pulse, 0.5 s acquisition time, and 10 s recycle delay, were used. The chemical shifts were calibrated using tetramethylsilane as an external reference. A stimulated spin echo (diffste) was used for the solutions from the diffusion experiments, using 16 scans in 16 gradient steps. The parameters included a  $\Delta = 50\ \text{ms}$  diffusion delay, a  $\delta = 1\ \text{ms}$  gradient pulse duration, and a  $g = 500\ \text{G/cm}$  maximum gradient strength. The gradient strength was calibrated against a reference (HDO signal in  $\text{D}_2\text{O}$  with  $D = 1.902 \cdot 10^{-9}\ \text{m}^2/\text{s}$  at 298 K) (Mills 1973). DOSY processing was performed in Mestrenova 14.1.2 using the Inverse Laplace method.

The self-diffusion coefficients were calculated by fitting the attenuation of the signal integral intensity from diffusion experiments to the Stejskal-Tanner equation (Stejskal and Tanner 1965):

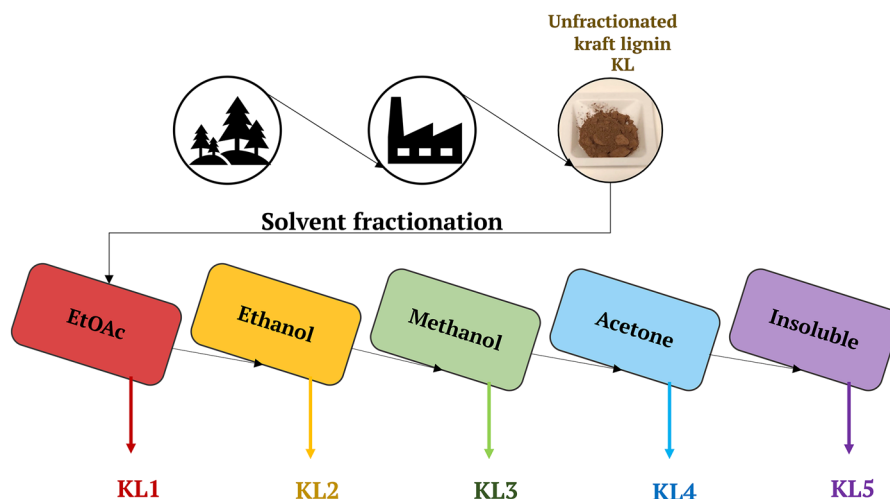
$$I = I_0 \exp \left\{ -D(\gamma g \delta)^2 \right\} (\Delta - \delta/3) \quad (1)$$

where  $I$  is the signal intensity,  $I_0$  the signal intensity at zero gradient strength,  $\gamma$  the gyromagnetic ratio of the nucleus studied, and  $g$  the variable gradient strength. The diffusion coefficients obtained were calibrated using a standard sample of pure  $\text{D}_2\text{O}$  (Holz and Weingartner 1991).

### $^{31}\text{P}$ -NMR spectroscopy

Functional group analysis was performed by  $^{31}\text{P}$ -NMR according to previously reported work (Argyropoulos 1994). 30 mg of the lyophilized lignin samples were accurately weighed and 200  $\mu\text{L}$  of dimethylformamide (DMF) and pyridine (1:1) were added. The solution was stirred for 30 min at  $50\ ^\circ\text{C}$ . Afterward, 50  $\mu\text{L}$  of the internal standard solution was added and the mixing continued for another 30 min. The internal standard solution comprised endo-*N*-Hydroxy-5-norbornene-2,3-dicarboximide (eHNDI) in pyridine (60 mg/mL) and contained 5 mg chromium (III) acetylacetonate per mL of pyridine. Finally, a solution of 100  $\mu\text{L}$  of 2-chloro-4,4,5,5-tetramethyl-1,3,2-dioxaphospholane and 450  $\mu\text{L}$  deuterated chloroform was added dropwise to the sample. The reaction proceeded for 60 min and the  $^{31}\text{P}$ -NMR spectrum was recorded immediately thereafter, with 256 scans and a D1 delay of 5 s. Assignment of the signals was reported according to previous work (Argyropoulos 1994). Measurements were performed in a Bruker

**Fig. 1** Schematic representation of the sequential solvent fractionation process. At each step lignin was dissolved in the mentioned solvent, stirred for 2 h and then filtered to be dissolved in the next solvent. Molecular weight of the fractionated samples is expected to increase from KL1 to KL5



Avanche III HD 400 MHz instrument equipped with a BBFO probe and a Z-gradient coil.

#### Experimental setup of the diffusion cells and procedure

Mass transfer experiments were performed using diffusion cells, as previously described (Ghaffari et al. 2022). The diffusion cells were custom-made PTFE cells, consisting of two half-cells. Each half-cell contained five cylindrical chambers of 15 mL volume. The half-cells were held together tightly, using screw rods, to ensure no leakages. RC membranes were placed between the cells and sealed with O-rings. To ensure homogeneity of solutions in the donor (containing lignin) and acceptor (containing blank solution) chambers and that the lignin diffusion to the surface of the membrane was not the rate-limiting step, the diffusion cells were placed on an orbital shaker (PSU-20i, LabTeamet, Grant Instruments, Cambridge, United Kingdom) operating at 100 rpm for the duration of the experiment. Donor solutions were prepared by dissolution of 100 mg of KL in 250 mL of NaOH solutions of 1, 0.1, and 0.01 M concentrations. The solutions were stirred for at least 2 h to ensure complete dissolution of KL. Visually clear solutions were obtained. The 50 kDa MWCO RC membranes were pretreated in 0.1 M NaOH solution for at least 1 h before starting the experiments and washed thoroughly with 0.1 M NaOH before mounting onto the diffusion cells. The diffusion cells setup was as follows: 15 mL of donor solution (containing lignin) and 15 mL of blank NaOH solution were simultaneously poured into the donor and acceptor chambers. 1 mL samples were collected from the acceptor chamber and replaced with the blank solution every 24 h for seven days. The replaced blank solution was accounted for in the calculations. The withdrawn acceptor samples were analyzed by UV/vis absorbance spectroscopy using a Cary60 UV–Vis spectrophotometer (Agilent Technologies, Inc., CA, USA). Cary WinUV scan application software (version 5.0.0.999, Agilent Technologies, Inc., CA, USA) was used for recording the spectra and device control. The samples were scanned from 600 to 200 nm at a rate of 4800 nm/min. The KL concentrations of the samples were quantified from sample absorbance at 280 nm based on a calibration curve of KL samples in

the concentration range of 10 to 40 mg/L. All diffusion experiments were conducted in triplicate.

#### Water permeation of RC membrane in various alkalinities

The water diffusion through 50 kDa MWCO RC membranes was measured using diffusion cells, according to the methodology previously described in the literature (Andersson et al. 2013). As described in the previous section, membranes were mounted between diffusion cells and 15 mL of NaOH solution (1, 0.1, or 0.01 M) was added simultaneously to each donor and acceptor compartment. 10  $\mu$ L of tritium-labeled water was added to the donor chamber and, at specific time intervals, 0.5 mL samples were withdrawn from the acceptor chamber and replaced immediately with 0.5 mL of deionized water. The diffusion cells were kept on an orbital shaker (75 rpm) at room temperature. The withdrawn samples were analyzed by a liquid scintillation analyzer (Tri-Carb B2810TR, Perkin–Elmer, USA). 3 mL of Ultima Gold solution was added to each sample prior to analysis. The experiments were conducted in triplicate. The mass transfer rate of water through the membrane was calculated using Eq. (2) derived by Van den Mooter et al. (Van den Mooter et al. 1994).

$$2(DS/hV)t = -\ln \left\{ (C_0 - 2C_a)/C_0 \right\} \quad (2)$$

where  $D$  ( $\text{m}^2 \text{s}^{-1}$ ) is the diffusion coefficient,  $S$  ( $\text{m}^2$ ) is the surface area of the membrane from which diffusion occurs, and  $V$  ( $\text{m}^3$ ) is the volumes of solution in the acceptor and donor chambers,  $h$  (m) is the thickness of the membrane,  $C_0$  and  $C_a$  ( $\text{g m}^{-3}$ ) are concentrations of the donor solution at the start and the acceptor solution at time  $t$ , respectively.

#### Size exclusion chromatography (SEC)

A SEC system (HPLC Pump 1515, Autosampler 717plus, Waters, Milford, MA, USA) was used to analyze the molecular weight of samples collected from donor and acceptor chambers of the diffusion cells. The separation was done through two analytical columns packed with Superdex 200 Increase (300 mm  $\times$  10 mm, 9  $\mu$ m) and Superdex 30 Increase (300  $\times$  10 mm, 9  $\mu$ m) (Cytiva, Uppsala, Sweden). 0.1 M NaOH (analytical grade) with a flow rate of

0.5 mL/min was used as the mobile phase and the column was operated at ambient temperature. For the calibration, polyethylene glycol (PEG) standards were used, ranging from 0.2 to 35 kDa (Merck Schuchardt OHG, Hohenbrunn, Germany). The system was equipped with a Waters 2414 refractive index (RI) detector and a Waters 2487 dual-wavelength UV detector, where the absorbances at wavelengths of 280 and 350 nm were used for detection.

## Results and discussion

This study aimed to investigate the influence of solution alkalinity on the diffusion of different fractionated KL samples through RC membranes. To interpret the results obtained from the diffusion cells, the starting material (unfractionated softwood KL) and the solvent-fractionated samples were characterized before being used in the diffusion cells.

### Characterization of the fractionated lignin samples

#### Content of hydroxyl groups

The content of hydroxyl groups in fractionated and unfractionated lignin was measured using  $^{31}\text{P}$ -NMR analysis, based on a method previously introduced by Argyropoulos (1994). The concentration of phenolic hydroxyls decreased with an increase in  $M_w$  of the fractions, indicating fewer end units in large  $M_w$  fractions (Table 1). In particular, the non-condensed phenolics (G-units in Table 1) support the observed decreasing trend. The trend is consistent with the cleavage of aryl ether linkages during pulping, which yielded smaller molecules with more free phenolic end groups. A reverse trend was observed

for carboxylic hydroxyls, suggesting that the lower molecular weight fractions were more prone to oxidation during the pulping, in agreement with current literature (Giummarella et al. 2020).

#### Molecular weight

SEC showed that the average molecular weights of different lignin samples in 0.1 M NaOH range from 1.9 to 10.8 kDa (see Table 1). Since these values were based on PEG standards, which, similar to many other standards, are not true representations of lignin molecules (Andrianova et al. 2018), these  $M_w$  values should only be regarded for comparison purposes between the different fractions. However, as expected, the results indicated a continuous increase in the average molecular weight from KL1 to KL5 (Duval and Lawoko 2014).

#### Lignin self-diffusion

The different lignin fraction molecular sizes in an organic solvent were examined by measuring the self-diffusion coefficients in DMSO- $d_6$ . Figure 2 shows the DOSY map, including the characteristic  $^1\text{H}$ -NMR peaks for lignin with KL1 on the top and KL5 on the bottom. The recorded self-diffusion coefficient varied from  $13.1 \cdot 10^{-11}$  to  $3.6 \cdot 10^{-11} \text{ m}^2 \text{ s}^{-1}$  for KL1 to KL5 (see table SI2). This agrees qualitatively well with the Stokes–Einstein law, stating that the diffusion coefficient is inversely proportional to the hydrodynamic radius of the diffusing species.

In diffusion NMR analysis, the samples were dissolved in DMSO- $d_6$ . This is, however, very different from the industrial processing conditions during kraft cooking and a question remains around how these fractions behave when dissolved in alkaline solutions.

**Table 1** Quantification of OH<sup>−</sup> functionalities of solvent-fractionated softwood KL samples by  $^{31}\text{P}$ -NMR analysis

Sample	Average molecular weights (kDa)	Aliphatic (mmol/g)	C5-substituted (mmol/g)	G-units (non-condensed) (mmol/g)	H-units (mmol/g)	Carboxylic (mmol/g)
KL	4.4	1.97	2.02	1.72	0.17	0.56
KL1	1.9	0.94	1.89	2.45	0.17	0.66
KL2	3.4	2.09	2.09	1.76	0.20	0.58
KL3	3.9	2.24	2.18	1.51	0.14	0.45
KL4	6.1	2.06	2.14	1.25	0.15	0.38
KL5	10.8	2.49	1.54	0.85	0.12	0.31

**Fig. 2** Five stacked DOSY NMR spectra of fractionated lignin in DMSO-d<sub>6</sub>

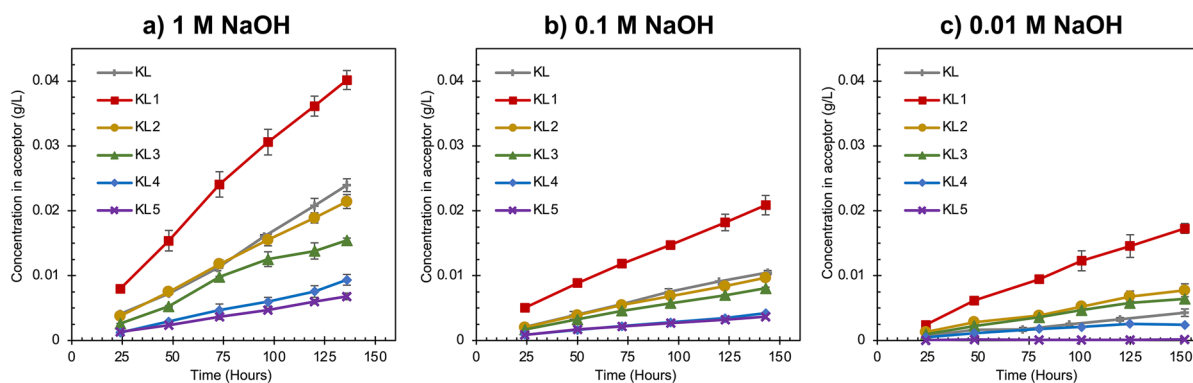
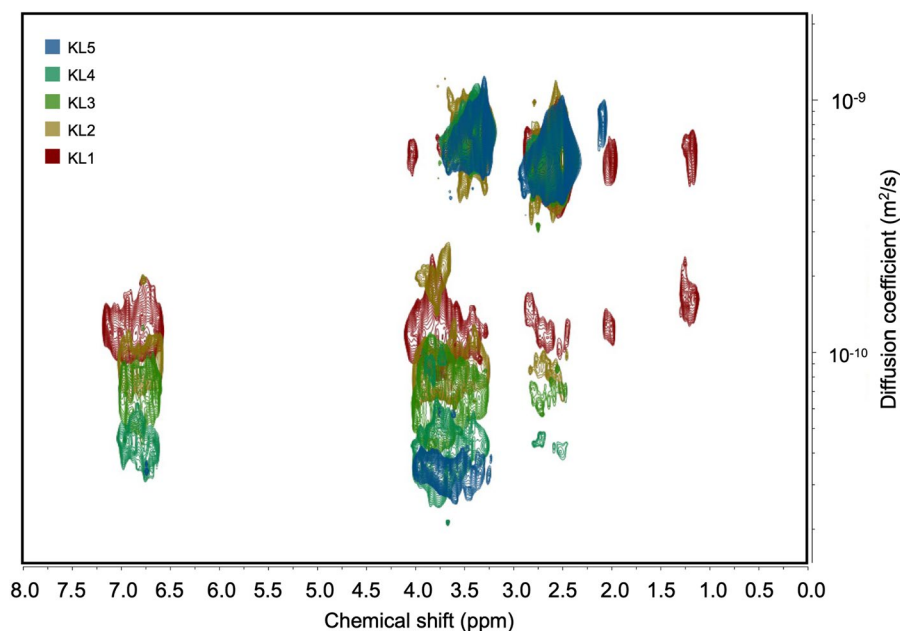


**Fig. 3** Concentration of lignin in acceptor chamber versus time in **a** 1 M NaOH solution; **b** 0.1 M NaOH solution; **c** 0.01 M NaOH solution. The lignin concentrations were deter-

mined by UV/Vis absorbance according to a calibration curve for softwood KL in alkaline solutions

Diffusion-cell experiments were therefore conducted to further elucidate this.

#### Transport through cellulose membranes

A key step in the lignification process is the transport of lignin out of the wood chip matrix. In this study, diffusion cells were used to investigate the transport behaviour of five lignin fractions at different alkalinities. The concentrations of the KL molecules transported through the membrane to the

acceptor chamber (referred to as “acceptor samples” from here on) were quantified by UV/Vis absorbance. The results can be seen in Fig. 3.

The concentration in the acceptor chamber increased linearly with time, no abrupt changes can be seen during the experiment for the three concentrations of NaOH (3). An increase in the transport rate from KL5 to KL1 was observed, which is in agreement with the data from the diffusion NMR experiments (Fig. 2). The systematically higher transport rates indicate a decrease in molecular

weight from KL5 to KL1, in agreement with the SEC experiments (Table 1).

There was an increased diffusivity with increased NaOH concentration for all fractions and the unfractionated sample. Increasing the NaOH concentration in the solution can affect the transport of lignin molecules in several ways. It has been shown that cellulose can swell in alkaline aqueous solutions (Grignon and Scallan 1980) and that the degree of swelling can cause a change in the size of the pores in the membrane. To confirm if the transport properties of the membrane change with alkalinity, water transport through the 50 kDa MWCO RC membrane was studied in deionized water and alkaline solutions in the range of 0 to 1 M NaOH (Fig. 4a). The water diffusivity increased by about 35% when the concentration of NaOH increased from 0 to 1 M, which could be due to either increased pore sizes or other changes in the membrane (Andersson et al. 2013). Interestingly, the lignin diffusivity increased by a factor of 3 to 5 (depending on the fractions) when the alkalinity increased from 0.01 M NaOH to 1 M NaOH (see Fig. 4b and Supplementary Information Table S13 for values). Therefore, the increase in membrane diffusivity due to swelling cannot solely account for the lignin transport rate changes. This indicates that the NaOH concentration also influences lignin molecules and/or their interactions with the membrane.

An increase in alkalinity affects lignin molecules in solution in various ways, one of which is by decreased association. It has been shown that when the concentration of  $\text{OH}^-$  ions in the solution

increases, the association of molecules decreases (Norgren et al. 2001). This is due to the higher charge of lignin molecules at higher alkalinities, resulting in an increased repulsion, thereby reducing the electrostatic association and preventing the formation of aggregates. The lignin molecules can also adsorb to the fully bleached softwood kraft pulp fibers, as previously suggested by Norgren and Bergfors (2005). If the lignin is adsorbed to the cellulose membrane surface, this can slow down its diffusion through the pores. The adsorption phenomenon is less likely to occur when the alkalinity of the solution is higher, due to the aforementioned reasons, meaning that the phenomenon is less pronounced when lignin is dissolved in a good solvent. It should be noted that as the ionic strength of the solution increases, the thickness of the electrostatic double layer decreases and the screening of charges increases (Berg 2010). However, how does the ionic strength affect the diffusion or adsorption of lignin molecules through the cellulose membrane pores is not discussed further in this study.

An increased transport rate was observed with increasing concentration of NaOH in the diffusion experiments, which could indicate decreasing sizes of the diffusion species. The association between KL molecules in highly alkaline solutions is limited, yet possible (Rudatin et al. 1989). In fact, Rudatin et al. (1989) reported indications of association between KL molecules even at pH levels around 13.5 when molecules were larger. The diffusivity of the unfractionated sample is located between KL1 and KL2 in 0.1 and 1 M NaOH, however, when alkalinity is

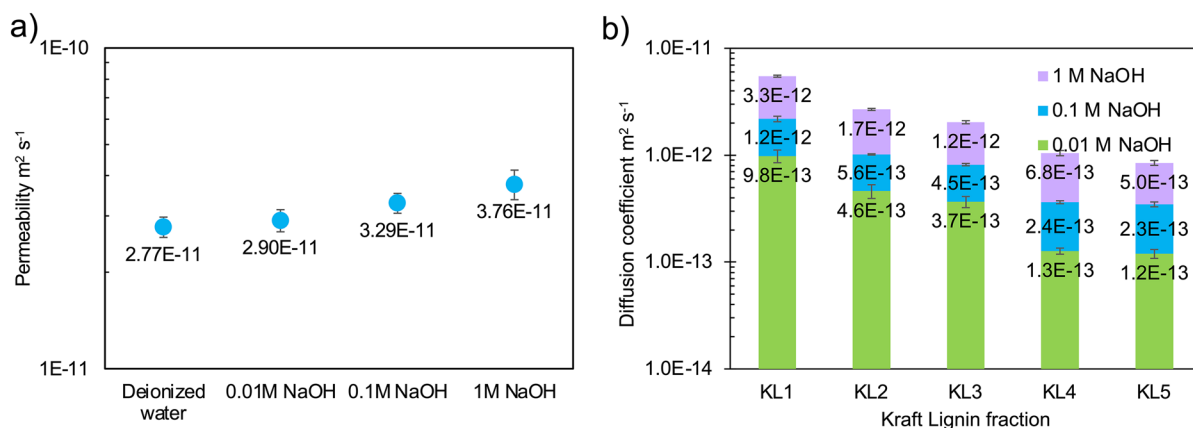


**Fig. 4** **a** Tritium-labeled water diffusivity of the 50 kDa MWCO membrane in different alkalinities; **b** Diffusivity of fractionated lignin in different alkalinities

lowered, the diffusivity of unfractionated sample is pushed toward larger  $M_w$  fractions indicating that more aggregates can be present in the lower alkalinity. When the alkalinity increased from 0.01 to 0.1 M NaOH, the diffusivity of fractions KL4 and KL5 improved by a factor of 1.9, while for the lower  $M_w$  fractions (KL1, KL2, KL3) this increase was by a factor of 1.2. This observation could be explained by the difference in association tendency for different fractions, i.e., lower association in the low  $M_w$  fractions. Since the association depends on the electrostatic interactions (repulsion), the degree of charging is an important factor when considering the association behaviour of the sample. Depending on the  $M_w$ , the  $pK_a$  of the phenolic groups changes (Norgren and Lindström 2000). If the  $M_w$  is higher, the  $pK_a$  value shifts towards higher alkalinity and the dissociation curve becomes flatter. This means that, at a certain alkalinity, the fraction of dissociated phenolic groups (charged molecules) is higher for small molecules than for large molecules (Norgren and Lindström 2000). Therefore, when alkalinity increased from 0.01 M NaOH, the increase in the number of charged molecules could be higher in the high  $M_w$  fractions since the low  $M_w$  species were mostly already charged at lower alkalinities.

Another possible explanation for the increased transport at 1 M NaOH could be that some of the lignin's native bonds break over time, forming low  $M_w$  fragments with higher diffusivity. This effect should be more pronounced for the high  $M_w$  fractions since they were less degraded by the pulping process (Crestini et al. 2017).

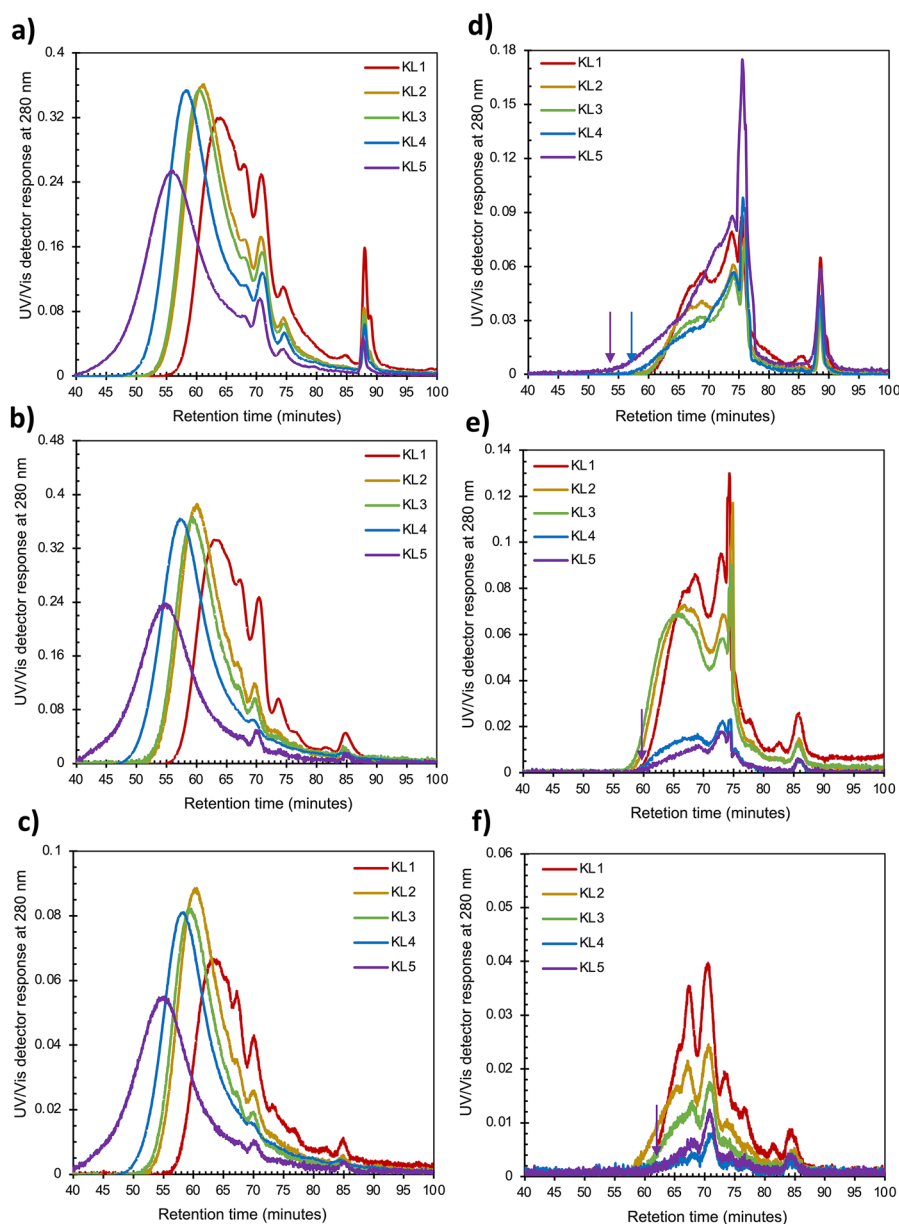
The  $M_w$  of the lignin molecules in the donor and acceptor chambers was determined using SEC at different alkalinities. However, as mentioned earlier lignin molecules can associate in alkaline solution and this association is sensitive to alkalinity level which can affect the SEC results where smaller  $M_w$  can be recorded for lignin molecules dissolved in higher alkalinity. The  $M_w$  value of the donor samples in 1 M NaOH was lower than that of the donor samples in 0.1 M or 0.01 M NaOH (values are presented in Table SI 1 in the supplementary information). This could be an indication of the formation of fewer aggregates or some degradation of molecules in 1 M NaOH. However, one should be aware that absolute  $M_w$  determinations of lignin are challenging. Therefore, for comparison purposes, the following

discussions are based on the retention times ( $R_T$ ) shown in the chromatograms.

Figure 5 shows all the chromatograms from the donor and acceptor samples at different NaOH concentrations. The overall shapes of the donor chromatograms for each fraction were similar at all NaOH concentrations, except for the peak at a retention time of around 74 min. This peak was visible for all KLs in the 1 M NaOH samples but, in the 0.1 M and 0.01 M solutions, it could only be observed for KL1. The 74-min-peak should represent molecules of sizes less than 0.5 kDa and it likely represents a degradation product of lignin at high NaOH concentrations. The KL1 sample contained most of the lowest molecular weight molecules, which explains why the 74 min-peak is present in KL1 graphs at all alkalinities. When the concentration of NaOH increases, native ether bonds in the molecules may break, generating smaller molecules. High alkalinity could also prevent potential associations and small lignin fragments could be released and detected in the SEC chromatogram. Independent of the reason, the larger proportion of small molecules in the 1 M NaOH samples can explain the higher transport rates of lignin at this alkalinity (see Fig. 6a, b for a schematic view of the effect of  $M_w$  on the lignin transport mechanism).

The SEC chromatograms for the acceptors are presented in Fig. 5d–f. All the 0.01 M acceptor samples had very low concentrations, therefore, their chromatograms appear noisier. Before, we showed that the transport rate of lignin over the membrane increased with increasing alkalinity but are all fractions affected similarly, or is the effect emphasized for some fractions more than others? The onset of the SEC curves correlates to the largest molecules that have been able to pass through the membrane during the diffusion experiment, which was unchanged for KL1, KL2, and KL3 when alkalinity was increased from 0.01 to 1 M NaOH. However, for KL4 and KL5, the onset of the curves is moved from about 60 min to shorter retention times, i.e., 57 and 54 min, respectively (see purple and blue arrows in Fig. 5d). This indicates that higher alkalinities facilitate the transport of larger molecules, whereas lower alkalinities hinder this transport. This could be explained by the association of KL molecules, previously suggested as a reason behind the slow diffusion of lignin through fiber walls (Li and Mui 1999; Mattsson et al. 2017). If the large lignin molecules associate with each other,

**Fig. 5** UV detector response of SEC at 280 nm for various fractions of KL in the donor chamber of diffusion cells in **a** 1 M NaOH; **b** 0.1 M NaOH; **c** 0.01 M NaOH, and in the acceptor chamber of **d** 1 M NaOH; **e** 0.1 M NaOH; **f** 0.01 M NaOH after 168 h

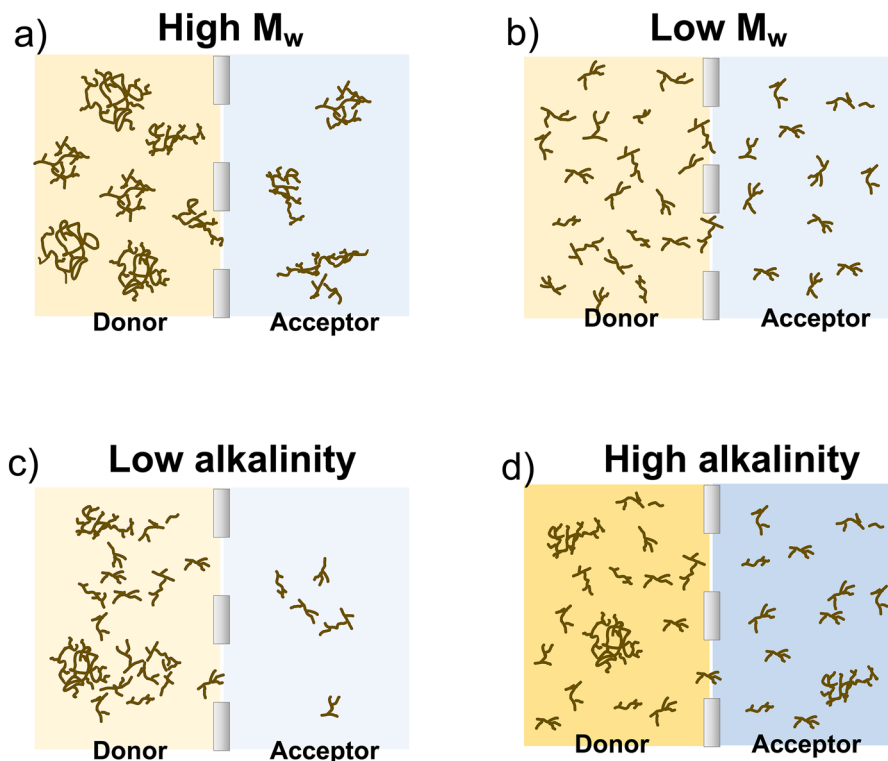


or with smaller lignin molecules, they could create loose clusters, which would significantly slow down their diffusion. Thus, they would not be detected in the SEC chromatograms of acceptor samples in low alkalinities.

The UV/Vis spectra from samples of varying alkalinity were compared to investigate whether there was a chemical difference between the samples. To enable a more straightforward interpretation, all the graphs have been normalized to absorbance at

300 nm, see Fig. 7. In the donor spectra, as the alkalinity decreased, the maximum moved from 300 nm to shorter wavelengths around 280 nm, which was more obviously observed for the higher  $M_w$  fractions like KL5. Furthermore, the donor spectra of the smaller  $M_w$  fractions (KL1 and KL2) showed higher absorbances around 350 nm in 1 M and 0.1 M NaOH compared to the higher  $M_w$  fractions. The UV/Vis spectra of the acceptor samples are shown in Fig. 7d, e, f, where they differ significantly from the

**Fig. 6** Schematic representation of comparing KL diffusion through the pores of the membrane when **a, b** the alkalinity of the solution is the same but  $M_w$  is different; **c, d**  $M_w$  is the same but alkalinity is different



donor spectra, having an additional peak at around 350 nm. The peak, with a shoulder at around 320 nm, increased with increasing NaOH concentration. At higher NaOH concentrations, i.e., 0.1 and 1 M, the maximum shifted from 280 to 300 nm, which was also more apparent in higher  $M_w$  fractions like KL5.

Previous studies have shown that the ionization of the hydroxyl groups could induce hyperchromic and bathochromic shifts in the UV/Vis spectrum (Goldmann et al. 2017). Lignin phenolic units with a conjugated bond in the  $\alpha$ -position of the aliphatic chain were shown to have an additional absorbance peak at around 350 nm when present in alkaline conditions. The acceptor spectra in Fig. 7 show that the peak at 350 nm is present at all three alkalinities and the relative intensity at 350 nm increases from KL1 to KL5.

The higher relative concentration of conjugated structures in the acceptor solution can be due to different possible reasons. Many lignin monomers or oligomers can have conjugated bonds in the aliphatic chain (Giummarella et al. 2020), which would show absorbance peaks at 350 nm, 320 nm, and 300 nm, depending on the concentration of NaOH in the solution (see isosbestic points and changes in UV/Vis

spectra with alkalinity for vanillin, as an example of a conjugated lignin monomer, in the Supplementary Information Fig. S11). The breaking of aryl-ether bonds to smaller molecules occurs through quinone methide intermediates. The formation of conjugated bonds on  $\alpha$  or  $\beta$  carbons results in the formation of conjugated phenolic end groups, which can be easily charged in alkaline solutions and show a peak at 350 nm (Sixta 2006; Crestini et al. 2017). The occurrence of peaks at 350 nm in the acceptor solutions indicates a larger ratio of smaller conjugated molecules to unconjugated molecules. Potentially, these smaller molecules, such as monomers and oligomers, are transported faster than the larger molecules.

In addition, for the acceptor samples at 0.01 M NaOH, the intensities for the 280 nm peaks of KL1 and KL2 were higher than for the 350 nm peaks, whereas intensities were more similar for the other fractions. This can be interpreted as the concentration of conjugated lignin units in KL1 and KL2 relative to the unconjugated ones being higher for 0.01 M samples.

Another observation was that the spectra for KL4 and KL5 at different alkalinities were more similar

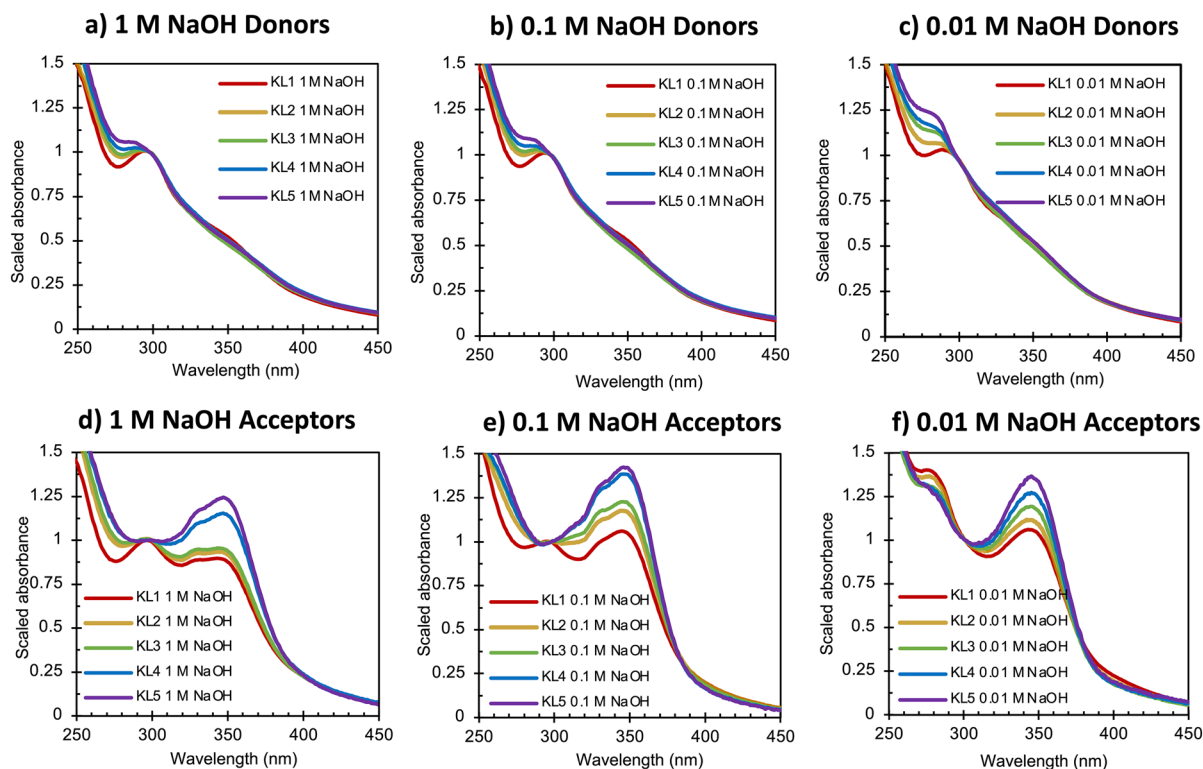


**Fig. 7** Normalized (to 1 at 300 nm) UV/Vis absorbance spectra of the donor (at the start) in **a** 1 M NaOH; **b** 0.01 M NaOH; **c** 0.01 M NaOH and acceptor (after 168 h) samples in **d** 1 M NaOH; **e** 0.1 M NaOH; **f** KL5 in 0.01 M NaOH

than those of KL4 and KL3. Thus, KL4 and KL5 seem to have a more chemically similar structure, in line with the  $^{31}\text{P}$ -NMR data. It is worth mentioning that the transport rate over the membranes and the SEC chromatograms for these two fractions also look very similar (see Fig. 3 and Fig. 5d–f).

## Conclusion

Diffusion cells were used to study the diffusional transport of lignin molecules with varying molecular weights through model cellulose membranes and in solutions with different alkalinities. The differences in the UV/Vis absorbance spectra between samples from the donor and acceptor chambers showed chemical fractionation occurring during the diffusion experiments for all solvent-fractionated samples. A distinct peak around 350 nm was observed in the acceptor samples. This peak correlates to conjugated lignin molecules at high alkalinities, where these groups

can be attributed to small molecules such as monomers and oligomers. As expected, higher molecular weight fractions exhibited lower transport rates but at higher alkalinities, the overall mass transport rates increased for all lignin molecules, with larger molecules exhibiting a more significant change. Based on these results, we propose the following reasons to explain the higher lignin transport rates at higher NaOH concentrations:

Dissociation of lignin aggregates at higher pH values could occur due to more charges on the molecules and higher electrostatic repulsion between the molecules.

Formation of small molecules could occur due to possibly slow degradation of lignin molecules at high alkalinities. The small molecules would pass through the membrane faster, therefore, their concentration would become enriched in the acceptor chamber. This was observed as a peak in the SEC chromatograms at 74 min for the 1 M NaOH samples.

Changes in the membranes could also account for the increased diffusivity of lignin. As shown, the diffusion of water over the membranes increases by increasing the concentration of NaOH, which is a sign that the membrane changes as alkalinity changes. This study was performed in a simplified setup and at room temperature, it should be noted that diffusion is a complex and temperature sensitive phenomena and by increasing the temperature the diffusion rate would increase, therefore, the results of this study should be interpreted with caution in regard to extrapolating to the pulping processes.

The current study has provided more detailed information on the diffusion of lignin in highly alkaline conditions than is available in existing literature. These findings can be employed in modern pulping processes to improve the available process for a better yield and higher efficiency.

**Acknowledgments** We would also want to thank Tuve Mattson for discussion when the project was initiated.

**Author contributions** RG and AL conceived the idea and designed the experiments. RG performed the experiments and analyzed the data with input from AL. SEC experiments were assisted by HA and the results of these experiments were discussed together with GL. Diffusion NMR spectroscopy was performed by AI, and the results were discussed together with LE. The  $^{31}\text{P}$ -NMR experiments were performed by IS, and together with ML the results were discussed. The original draft of the manuscript was written by RG and AL. All the authors discussed the results and edited the manuscript before giving their approval to the final version.

**Funding** Open access funding provided by Chalmers University of Technology. This research was funded by Knut and Alice Wallenberg Foundation, through the Wallenberg Wood Science Center (WWSC), BIOINNOVATION, VINNOVA, Sweden and FibRe—Design for circularity—Lignocellulose-based thermoplastics (Grant Number 2019-00047), a VINNOVA competence center for financial support.

## Declarations

**Conflict of interest** The authors declare no conflict of interest.

**Open Access** This article is licensed under a Creative Commons Attribution 4.0 International License, which permits use, sharing, adaptation, distribution and reproduction in any medium or format, as long as you give appropriate credit to the original author(s) and the source, provide a link to the Creative Commons licence, and indicate if changes were made. The images or other third party material in this article are included in the article's Creative Commons licence, unless indicated otherwise in a credit line to the material. If material is not

included in the article's Creative Commons licence and your intended use is not permitted by statutory regulation or exceeds the permitted use, you will need to obtain permission directly from the copyright holder. To view a copy of this licence, visit <http://creativecommons.org/licenses/by/4.0/>.

## References

- Andersson H, Hjartstam J, Stading M et al (2013) Effects of molecular weight on permeability and microstructure of mixed ethyl-hydroxypropyl-cellulose films. *Eur J Pharm Sci* 48:240–248. <https://doi.org/10.1016/j.ejps.2012.11.003>
- Andrianova AA, Yeudakimenka NA, Lilak SL et al (2018) Size exclusion chromatography of lignin: The mechanistic aspects and elimination of undesired secondary interactions. *J Chromatogr A* 1534:101–110. <https://doi.org/10.1016/j.chroma.2017.12.051>
- Argyropoulos DS (1994) Quantitative phosphorus-31 NMR analysis of lignins, a new tool for the lignin chemist. *J Wood Chem Technol* 14:45–63. <https://doi.org/10.1080/02773819408003085>
- Berg JC (2010) An introduction to interfaces & colloids: the bridge to nanoscience. World Scientific, pp 466–483
- Birch MA, Kozhin VP, Shchitnikov VK (1999) Kinetics of wood impregnation process. *J Eng Phys Thermophys* 72:618–626
- Bogren J, Brelid H, Theliander H (2007) Reaction kinetics of softwood kraft delignification—General considerations and experimental data. *Nord Pulp Pap Res J* 22:177–183. <https://doi.org/10.3183/npprj-2007-22-02-p177-183>
- Brännvall E, Rönnols J (2021) Analysis of entrapped and free liquor to gain new insights into kraft pulping. *Cellulose* 28:2403–2418. <https://doi.org/10.1007/s10570-020-03651-3>
- Crestini C, Lange H, Sette M, Argyropoulos DS (2017) On the structure of softwood kraft lignin. *Green Chem* 19:4104–4121. <https://doi.org/10.1039/c7gc01812f>
- Dutta S, Garver TM, Sarkanen S (1989) Modes of association between kraft lignin components. *Lignin* 397:155–176. <https://doi.org/10.1021/bk-1989-0397.ch012>
- Duval A, Lawoko M (2014) A review on lignin-based polymeric, micro- and nano-structured materials. *React Funct Polym* 85:78–96. <https://doi.org/10.1016/j.reactfunctpolym.2014.09.017>
- Duval A, Vilaplana F, Crestini C, Lawoko M (2016) Solvent screening for the fractionation of industrial kraft lignin. *Holzforschung* 70:11–20. <https://doi.org/10.1515/hf-2014-0346>
- Favis BD, Choi PMK, Adler PM, Goring DAI (1981) Leaching of lignin from unbleached kraft fibers suspended in water. *Pulp Pap CANADA* 82:TR35–TR40
- Ghaffari R, Almqvist H, Nilsson R et al (2022) Mass transport of lignin in confined pores. *Polymers (Basel)*. <https://doi.org/10.3390/polym14101993>
- Gierer J (1980) Chemical aspects of kraft pulping. *Wood Sci Technol* 14:241–266. <https://doi.org/10.1007/BF00383453>

- Giummarella N, Lindén PA, Areskog D, Lawoko M (2020) Fractional profiling of kraft lignin structure: unravelling insights on lignin reaction mechanisms. *ACS Sustain Chem Eng* 8:1112–1120. <https://doi.org/10.1021/acsschemeng.9b06027>
- Goldmann WM, Ahola J, Mankinen O et al (2017) Determination of phenolic hydroxyl groups in technical lignins by ionization difference ultraviolet spectrophotometry ( $\Delta\epsilon$ -IDUS method). *Period Polytech Chem Eng* 61:93–101. <https://doi.org/10.3311/PPCh.9269>
- Grignon J, Scallan AM (1980) Effect of pH and neutral salts upon the swelling of cellulose gels. *J Appl Polym Sci* 25:2829–2843. <https://doi.org/10.1002/app.1980.070251215>
- Gustafson RR (1988) Role of diffusion during initial delignification of alkaline pulping. *Tappi J* 71:145–147
- Holz M, Weingartner H (1991) Calibration in accurate spin-echo self-diffusion measurements using  $^1\text{H}$  and less-common nuclei. *J Magn Reson* 92:115–125. [https://doi.org/10.1016/0022-2364\(91\)90252-O](https://doi.org/10.1016/0022-2364(91)90252-O)
- Kawamata Y, Yoshikawa T, Aoki H et al (2019) Kinetic analysis of delignification of cedar wood during organosolv treatment with a two-phase solvent using the unreacted-core model. *Chem Eng J* 368:71–78. <https://doi.org/10.1016/j.cej.2019.02.103>
- Kolavali R, Theliander H (2013) Determination of the diffusion of monovalent cations into wood under isothermal conditions based on LiCl impregnation of Norway spruce. *Holzforschung* 67:559–565. <https://doi.org/10.1515/hf-2012-0182>
- Komatsu T, Yokoyama T (2021) Revisiting the condensation reaction of lignin in alkaline pulping with quantitativity part I: the simplest condensation between vanillyl alcohol and creosol under soda cooking conditions. *J Wood Sci.* <https://doi.org/10.1186/s10086-021-01978-4>
- Li J, Macleod JM (1993) Alkaline leaching of kraft pulps for lignin removal. *J Pulp Pap Sci* 19:85–92
- Li J, Mui C (1999) Effect of lignin diffusion on kraft delignification kinetics as determined by liquor analysis. Part I: an experimental study. *J Pulp Pap Sci* 25:373–377
- Li J, Phoenix A, Macleod JM (1997) Diffusion of lignin macromolecules within the fibre walls of kraft pulp. Part I: determination of the diffusion coefficient under alkaline conditions. *Can J Chem Eng* 75:16–22. <https://doi.org/10.1002/cjce.5450750105>
- Lindgren CT, Lindström ME (1997) The kinetics of residual delignification and factors affecting the amount of residual lignin during kraft pulping. *Nord Pulp Pap Res J* 12:124–127
- Mattsson C, Hasani M, Dang B et al (2017) About structural changes of lignin during kraft cooking and the kinetics of delignification. *Holzforschung* 71:545–553. <https://doi.org/10.1515/hf-2016-0190>
- Mills R (1973) Self-diffusion in normal and heavy water in the range 1–45°. *J Phys Chem* 77:685–688. <https://doi.org/10.1021/j100624a025>
- Norgren M, Lindström B (2000) Dissociation of phenolic groups in kraft lignin at elevated temperatures. *Holz-forschung* 54:519–527. <https://doi.org/10.1515/HF.2000.088>
- Norgren M, Bergfors E (2005) Sorption of kraft lignin from spent liquors on pulp fibres. *Wood Sci Technol* 39:512–520. <https://doi.org/10.1007/s00226-005-0008-y>
- Norgren M, Edlund H, Wågberg L et al (2001) Aggregation of kraft lignin derivatives under conditions relevant to the process, part I: phase behaviour. *Colloids Surf A Physicochem Eng Asp* 194:85–96. [https://doi.org/10.1016/S0927-7757\(01\)00753-1](https://doi.org/10.1016/S0927-7757(01)00753-1)
- Norgren M, Edlund H, Wågberg L (2002) Aggregation of lignin derivatives under alkaline conditions Kinetics and aggregate structure. *Langmuir* 18:2859–2865. <https://doi.org/10.1021/la011627d>
- Raiford DS, Fisk CL, Becker ED (1979) Calibration of methanol and ethylene glycol nuclear magnetic resonance thermometers. *Anal Chem* 51:2050–2051. <https://doi.org/10.1021/ac50048a040>
- Rudatin S, Sen YL, Woerner DL (1989) Association of kraft lignin in aqueous solution. In: *Lignin*. American Chemical Society, pp 144–154. <https://doi.org/10.1021/bk-1989-0397.ch011>
- Sixta H (2006) *Handbook of pulp*, vol 2. pp 109–164
- Stejskal EO, Tanner JE (1965) Spin diffusion measurements: spin echoes in the presence of a time-dependent field gradient. *J Chem Phys* 42:288–292. <https://doi.org/10.1063/1.1695690>
- Vainio U, Maximova N, Hortling B et al (2004) Morphology of dry lignins and size and shape of dissolved kraft lignin particles by X-ray scattering. *Langmuir* 20:9736–9744. <https://doi.org/10.1021/la048407v>
- Van den Mooter G, Samyn C, Kinget R (1994) Characterization of colon-specific azo polymers: a study of the swelling properties and the permeability of isolated polymer films. *Int J Pharm* 111:127–136. [https://doi.org/10.1016/0378-5173\(94\)00102-2](https://doi.org/10.1016/0378-5173(94)00102-2)

**Publisher's Note** Springer Nature remains neutral with regard to jurisdictional claims in published maps and institutional affiliations.